Swelling and annealing phenomena of Si crystal irradiated by Ar and C ion beams

J. Zhang[1], S. Momota[1], T. Toyonaga[1], H. Terauchi[1], F. Imanishi[1], J. Taniguchi[2]
[1]Department of Mechanical Systems Engineering, Kochi University of Technology
[2]Department of Applied Electronics, Tokyo University of Science
E-mail: 138005y@gs.kochi-tech.ac.jp

Abstract

The swelling phenomenon of Si crystal, irradiated by Ar^+ and C^+ beams, and its morphological change through the thermal annealing process have been studied. The height of swelling structures produced by the Ar^+ beam is much higher than that produced by the C^+ beam at energy 90 keV with the fluence up to $8\times10^{16}/cm^2$. The large different in the swelling height was well understood base on the productivity of vacancies evaluated by the SRIM simulation and experiment. Post-implantation samples irradiated with fluence $4\times10^{16}/cm^2$, were annealed at various temperatures in the range of 200 ～ 800 ℃. In the case of Ar^+ irradiated samples, the swelling height started to increase at about 600 ℃. In contrast, in the case of C^+ beam irradiated samples, the swelling height started to decrease at about 600 ℃ and almost disappeared at 800 ℃. The opposite behavior is understood based on the difference in irradiation-induced defect and in rearrangement mechanism in the thermal annealing process.

Keyword: swelling height, argon beam, carbon beam, silicon, simulation, annealing

1. Introduction

An irradiation of ion beams can produce damage in a crystal. The damage shows various features corresponding to irradiation parameters, such as the energy, fluence, angle, ion species and temperature etc. This damage causes relevant morphological changes on the irradiated crystals, for example, surface swelling and milling. In previous studies, it was found that ion beam irradiation can induce a swelling phenomenon on crystal materials [1; 2]. This swelling effect has been obtained in a great number of different semiconductors and insulators such as Si, Ge, SiC, GaAs, GaN, MgO, $LiNbO_3$, Al_2O_3, LiF, etc. The behaviors of these swelling processes are related to the materials and irradiation parameters [3].

Silicon is one of the popular materials in the semiconductor industry, while the swelling effects studied on silicon were primary valued the host ion beam of medium energy irradiated [4] or the high energy irradiated Si target [5; 6]. Although a successful application of the swelling phenomenon relies on understanding the swelling mechanism, the experimental studies to disclose the the swelling effect is not sufficient. The swelling phenomenon would be also useful object to investigate irradiation effect of ion beams through the systematic study.

In the present work, we have observed the fluence dependence of the Si swelling height, which had been induced by Ar and C beams under a same experimental condition. The annealing method was also performed to study the rearrangement of defect induced in Si crystal. The swelling mechanism will be discussed by considering the different swelling and annealing features found in the present results, and by comparing with defect distribution provide by a simulation code.

2. Experimental

Single-crystal Si (100) samples of thickness 0.5 mm with a size of 1 × 1 cm^2 were used to observe the swelling experiment. Before bombardment, all of the samples were cleaned by HF acid and then soaked in ultra-pure water. The chemical treatment was performed to remove the oxidized layer on the Si crystal. Irradiation experiments were performed by Ar^+ and C^+ ions, respectively. The ions were implanted into Si samples with a fluence range from 0.5×10^{16} to $8\times10^{16}/cm^2$ with a fixed energy 90 keV. Ar and C ions were implanted in a vacuum chamber (6.0×10^{7}~7.0×10^{7} Pa) at room temperature (RT) with normal incidence through a 100 μm striped stencil mask made of stainless steel. The mask has constant stripes, whose length and width are 2.0 mm and 0.13 mm. Owing to the masks, a portion of the irradiated areas were shielded and other areas were exposed by the mask strips to ion beam irradiation. It is convenient to quantify the swelling effect by a direct comparison with the virgin area. The ion beam bombardment experiments were performed by a 10-GHz NANOGAN, which is an ECR ion source installed at Kochi University of Technology. The machine was described elsewhere [7]. The post-irradiated samples of $4\times10^{16}/cm^2$ were annealed in an argon ambient environment at atmospheric pressure. The annealed temperature was in the range of 200 ～ 800 ℃ in steps of 200 ℃ and the annealing time was fixed at 60 min per step. The profile of the surface pattern was measured by using a α-step IQ surface profiler. The results measured by the α-step were consistent with those observed by atomic force microscopy (AFM) within an accuracy of about ±5 nm. Fig. 1(a) shows an image around the border between the implanted and un-implanted area measured by AFM. A swelling structure can be clearly seen at the implanted area in the figure. Fig. 1(b) shows a profile surface of the swelling structures measured by α-step. In this figure, the top part and the bottom part correspond to the implanted part and the un-implanted part, respectively. The swelling height is defined the distance between the averaged levels of the implanted and un-implanted parts in the stripes.

3. Result and Discussion

3.1 Simulation

SRIM 2008 calculations were performed for both ion irradiations (full cascade simulations) [8]. The Si target of density 2.321 g/cm^3 and the threshold displacement energy of 15eV were used in the calculation. We calculated the range of ions at 90 keV and the dpa (displacement per atom) distribution at a depth corresponding to the ion fluencies, which are show in Fig. 2. The irradiated depths of the Ar and C ions were inhomogeneous. The project ranges of Ar and C beams were 99.1 nm and 256.6 nm, respectively. The dpa values increase with increasing the fluence of both kinds of ions. For the case of a uniform fluence, the Ar beam could produce a larger number of displaced Si atoms than the C beam. We can understand that, at the same irradiation parameters, Ar beam can induce larger number of damage than the C beam. Simulation also provides mean values of the irradiation by the Ar and C beams in Table. 1. In $(-dE/dX)_e$ and $(-dE/dX)_n$ values, the Ar nuclear stopping power is larger than the electronic stopping power. However, the C beam nuclear stopping power is about one sixth of the electronic stopping power. This means that most of the C ion energy is lost due to electron collision. Comparing the two ions, they are obvious in different collision effects. The Ar beam can produce larger damage than the C beam in the Si target under the same irradiation condition.

3.2 Swelling results

SRIM calculates how ions stop in a thin top layer of a Si crystal. The expansion effect is observed at the irradiated area in experiment. Fig. 3 shows the swelling height as a function of the fluence irradiated by Ar^+ and C^+ beams with energy of 90 keV, which is larger than the threshold energies. The error bars in the figure show the standard deviation of the observed height of the swelling structure.

Concerning the Ar^+ irradiated swelling height, the fluence range was $10^{16}/cm^2$ ～ $8\times10^{16}/cm^2$ and the swelling height that increased up to about 60 nm. The swelling height increases with increasing the fluence. The irradiated Ar atoms accumulated is accounted for a few percentage for the swelling height by the calculation, that the swelling height has a strong relation with irradiated damage. The numbers of disorder atoms increased, when we increased the irradiation fluence [9]. In the C^+ irradiated swelling height, the fluence range was $5\times10^{15}/cm^2$ ～ $4\times10^{16}/cm^2$ and the swelling height was a few nanometer about 5 nm. C beam irradiation induces amorphous Si and $Si_{1-x}C_x$ amorphous alloy states. The transformation of a given volume of crystal Si into Si-C compounds does not involve a larger change of the Si atomic density, but requires mainly the addition of a sufficient number of C atoms to the lattice and some atomic rearrangement, besides the emission of a few silicon self-interstitials Si_I [10]. Therefore the swelling height mainly comes from amorphous Si irradiated by the C beam. These two results are consistently understood with the nuclear stopping power contribution calculated by SRIM. In the same irradiation parameter, the Ar beam irradiated Si presents higher swelling height than the C beam.

3.3 Annealing results

Images of the annealed swelling structures are shown in Fig. 4. Four strip traces in the figures indicate the irradiated region. The annealing temperature is from 200 to 800 ℃ in steps of 200 ℃. In the case of Ar^+ beam irradiation, the irradiated pattern remains up to 800 ℃, as shown in Fig. 4(a). In contrast, in the case of C beam irradiation, the contrast of the irradiated pattern becomes weak at 600 ℃, and disappears after annealing at 800 ℃, as shown in Fig. 4(b). The Ar and C irradiated Si samples present different annealed appearances.

Fig. 5 shows the effect of annealing the swelling of Si samples (Ar^{1+} and C^{1+} irradiated Si, $4\times10^{16}/cm^2$ and 90keV) at various temperatures. For the different samples, the characteristics for the swelling height were observed with step-by-step annealing at various temperatures. The swelling height does not give rise to any measured changes until being annealed up to 400 ℃ for both samples. In Ar irradiated sample, the swelling height increased sharply at a temperature of 600 ℃ and increased further at 800 ℃. However, In the C irradiated sample, the swelling height decreased at 600 ℃, and the swelling height was almost close to the contributed swelling height of implanted C ions at 800 ℃. The extra height of C^+ irradiated sample in the annealed sample at 800 ℃ could be related to the amorphous $Si_{1-x}C_x$ alloy [11].

The different annealing phenomena were shown in the Ar and C beams irradiated Si samples. Ar^+ beam irradiated Si sample, under irradiation condition of 90 keV and $4\times10^{16}/cm^2$, can be formed a thick amorphous Si layer with Ar bubbles and voids [12;

13]. During the annealing process, the amorphous of Si was recovered by annealing [14; 15], but the Ar atoms were stable in Si until being annealed at a high temperature [16; 17]. In the previous study, the Ar bubble size remains almost constant at low temperature and increases sharply in a temperature range where the amorphous silicon starts to grow epitaxially. Si sample were further annealed at higher temperatures at which point the bubbles grew a little size as studied by Revesz et al. [18].

Fig. 6 shows the Ar irradiated Si sample surface after annealed 800 ℃. There are same regular nano-pits on the surface, and the average diameter is about 800 nm. The Ar atom has a low solubility in Si, it can escape from a Si crystal at high temperature [17]. These pits must be the Ar pores which bubbles diffuse from implanted position to the Si surface. These structures indicate there are Ar bubbles in the Si. These pore structures also contribute to the swelling height and they are not recovered during 800 ℃ annealing. The swelling height increases may suggest by bubble diffusion to the Si surface at annealed 600 ℃.

The C^+ beam irradiated Si sample had the different annealing characteristics and mechanisms from the Ar beam irradiated one. The swelling height does not show any evident measureable change until 400 ℃. Nevertheless, a significant reductive tendency of the swelling height was observed annealed at 600 ℃, and continued to reduce further when annealed at 800 ℃. In the C beam irradiated Si target, there are c-Si, amorphous Si and $Si_{1-x}C_x$ amorphous alloy states [19]. In the implanted Si samples layer, during the annealing process, the amorphous Si is recovered [14; 15], and the C atoms are diffused in silicon at 800 ℃, as observed by Werner et al. [20]. The swelling height decreased can be explained by recovering a recrystallisation process. During the annealing process, the amorphous layer transforms into an $Si_{1-x}C_x$ amorphous alloy mixed with a small quality of SiC [10; 11]. The transformation of amorphous Si into crystal Si and $Si_{1-x}C_x$ alloy induces the change of a decrease in the volume, so the swelling height decreases upon being annealed at high temperature.

4. Conclusion

The swelling height of Si crystal, induced by Ar^+ and C^+ ion beam, and its modification through post-irradiation annealing process have been observed. Based on experimental results, the mechanism of swelling and annealing phenomena has been discussed. The different features between Ar^+ and C^+ ion beams were understood by means of damage induced in Si crystal, which is evaluated by using simulation method calculates the damage of a Si crystal. Because of larger nuclear collision power of Ar beam compared with C beam, Ar beam have higher productivity of ion-beam induced damage in Si crystal under the same irradiation condition. Higher swelling height observed for Ar beam is understood the difference in the productivity of damage. In case of Ar beam, the damage induced in Si crystal is amorphous phase of Si, voids and small bubbles. In case of C beam, the damage induced in Si crystal is amorphous phase of Si and $Si_{1-x}C_x$ alloys and a little SiC, which would provide small contribution for volume expansion. The different features were also found in annealing process for Si crystals, irradiated by Ar and C ion beam with the fluence of $4\times10^{16}/cm^2$. The swelling height of the Ar irradiated Si crystal showed sudden increase at 600 ℃, and a small increase of the height occurred at 800 ℃. On the other hand, the swelling height of C irradiated Si crystal showed sudden decrease at 600℃ and was almost disappeared at 800 ℃. It is implied that the different annealing features would be understood by means of rearrangement process for amorphous phase of Si, which is almost recrystallized at 800 ℃. The Ar atom could exist in Si crystal as bubbles, which can change size corresponding to temperature. The swelling height would increase with increasing bubble size. In case of C ion beam, irradiated C atoms would diffuse, and forms $Si_{1-x}C_x$ amorphous alloys at high temperatures. The phase transfer from amorphous to crystal would cause the reduction in volume of the swelling area. These morphological measurement and annealing methods are useful to study the crystal swelling phenomenon and mechanism. It is needed to get the cross section image of the irradiated region to further study mechanisms in detail.

Reference:

[1] O.W. Holland, B.R. Appleton, J. Narayan, J. Appl. Phys. 54 (1983) 2295.

[2] C. Ascheron, A. Schindler, R. Flagmeyer, G. Otto, Nucl. Instr. and Meth. in Phys. Res. B 36 (1989) 163-172.

[3] S. Momota, J. Zhang, T. Toyonaga, H. Terauchi, K. Maeda, J. Taniguchi, T. Hirao, M. Furuta, T. kawaharamura, J. Nanosci. Nanotechnol (2011) In press.

[4] P. Giri, V. Raineri, G. Franzo, E. Rimini, Phys. Rev. B 65 (2001) 012110.

[5] M. Ikeyama, K. Saitoh, S. Nakao, H. Niwa, S. Tanemura, Y. Miyagawa, S. Miyagawa, 1998 International Conference on Ion Implantation Technology Proceedings 2 (1999) 736-739.

[6] J.S. Custer, M.O. Thompson, D.C. Jacobson, J.M. Poate, S. Roorda, W.C. Sinke, F. Spaepen, Appl. Phys. Lett. 64 (1994) 437.

[7] S. Momota, Y. Nojiri, M. Saihara, A. Sakamoto, H. Hamagawa, K. Hamaguchi, Rev. Sci. Instr. 75 (2004) 1497.

[8] J.F. Ziegler, J.P. Biersack, U. Littmark, The Stopping and Range of Ions in Solids (Pergamon, New York, 1985) (http://www.srim.org/).

[9] S.-i. Satake, S. Momota, S. Yamashina, M. Shibahara, J. Taniguchi, J. Appl. Phys. 106 (2009) 044910.

[10] J.K.N. Lindner, Appl. Phys. A 77 (2003) 27-38.

[11] W. Skorupa, A. Yankov, Materials Chemistry and Physics 44 (1996) 101-144.

[12] W.M. Lau, I. Bello, L.J. Huang, X. Feng, J. Appl. Phys. 74 (1993) 7101.

[13] T.K. Chini, D.P. Datta, U. Luchhesi, A. Mücklich, Surface and Coatings Technology 203 (2009) 2690-2693.

[14] H. Isogai, E. Toyoda, T. Senda, K. Izunome, K. Kashima, N. Toyoda, I. Yamada, Nucl. Instr. and Meth. in Phys. Res. B 257 (2007) 683-686.

[15] B. Li, C. Zhang, L. Zhou, Y. Yang, H. Zhang, Nucl. Instr. and Meth. in Phys. Res. B 266 (2008) 5112-5115.

[16] T.E. Seidel, R.L. Meek, A.G. Cullis, J. Appl. Phys. 46 (1975) 600.

[17] U. Bangert, P.J. Goodhew, C. Jeynes, I.H. Wilson, J. Phys. D 19 (1986) 589-603.

[18] P. Revesz, M. Wittmer, J. Roth, J.W. Mayer, J. Appl. Phys. 49 (1978) 5199.

[19] M.V. Nguyen, K. Vedam, J. Appl. Phys. 67 (1990) 3555.

[20] P. Werner, H.-J. Gossmann, D.C. Jacobson, U. Gösele, Appl. Phys. Lett. 73 (1998) 2465.

Table 1. Project range (R_p), mean electronic stopping power $(-dE/dX)_e$, mean nuclear stopping power $(-dE/dX)_n$ of ions in Si. The average number of displaced atoms per ion and per path length unit (dN_d/dx), calculated by SRIM2008.

Ion	Energy (keV)	R_p (nm)	$(-dE/dX)_e$ (keV/nm)	$(-dE/dX)_n$ (keV/nm)	dN_d/dx (/ion/nm)
Ar^+	90	99.12	0.3479	0.4911	1.78
C^+	90	256.6	0.2869	0.0451	2.97

Figure Caption

Figure 1. Swelling structure of an irradiated Si crystal observed by (a)AFM and (b) α-step. The beam fluence is $4\times10^{16}/cm^2$ and the energy is 90 keV.

Figure 2. (a) Depth contribution of Dpa induced by various Ar^{1+} ions and range. (b) Depth contribution of Dpa induced by various C^{1+} ion and range.

Figure 3. Swelling height as a function of the fluence irradiated by Ar^{1+} and C^{1+} ions.

Figure 4. An annealed images of the swelling structures. (a) Ar^{1+} irradiated Si. (b) C^{1+} irradiated Si

Figure 5. Swelling height of annealed Ar and C irradiated Si samples as a function of various temperatures.

Figure 6. 3-D AFM image of Ar pores on the Si surface for annealed 800 ℃.

Figure. 1

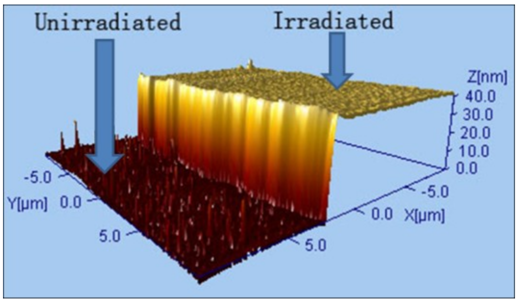

Unirradiated
Irradiated
Z[nm]
40.0
30.0
20.0
10.0
0.0
-5.0
Y[µm]
0.0
5.0
-5.0
0.0
X[µm]
5.0

(a)

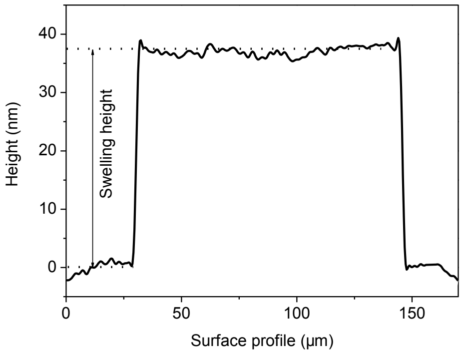

Height (nm)
Swelling height
40
30
20
10
0
0
50
100
150
Surface profile (µm)

(b)

Figure. 2

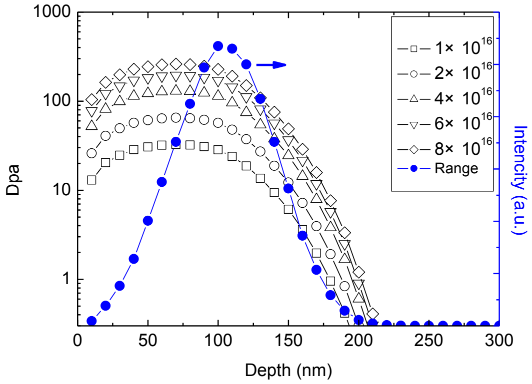

1000
100
10
1
Dpa
0
50
100
150
200
250
300
Depth (nm)
Intencity (a.u.)
1× 10^16
2× 10^16
4× 10^16
6× 10^16
8× 10^16
Range

(a)

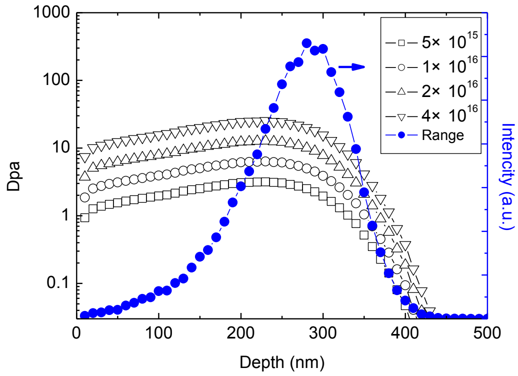

1000
100
10
1
0.1
Dpa
0
100
200
300
400
500
Depth (nm)
Intencity (a.u.)
5× 10^15
1× 10^16
2× 10^16
4× 10^16
Range

(b)

Figure. 3

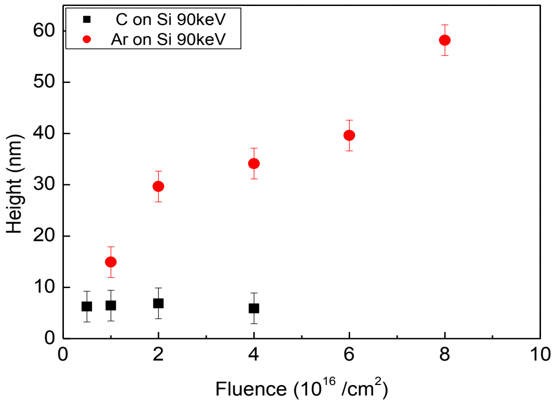
C on Si 90keV
Ar on Si 90keV
Height (nm)
0
10
20
30
40
50
60
0
2
4
6
8
10
Fluence (10^16 /cm^2)

Figure. 4

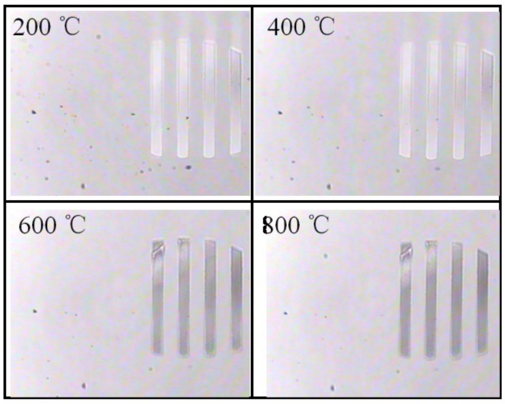

(a)

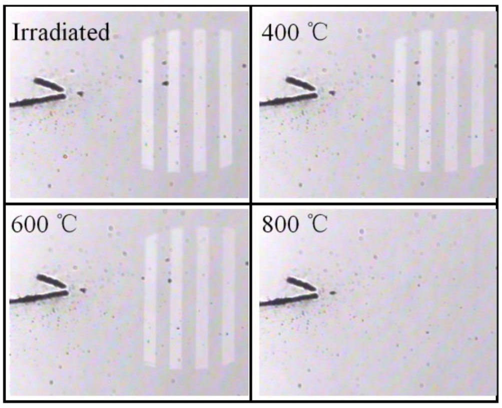

(b)

Figure. 5

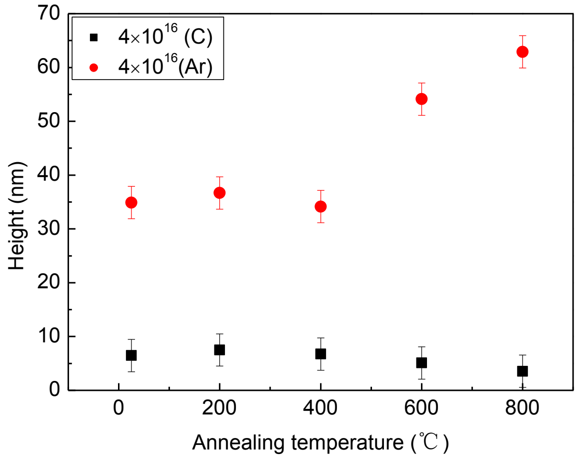

70
60
50
40
30
20
10
0
Height (nm)
4×10^16 (C)
4×10^16(Ar)
0
200
400
600
800
Annealing temperature (℃)

Figure. 6